Research Note

The Effects of Soil-Structure Interaction on Seismic Response of Steel Moment Resisting Frames

Sahand Jabini Asli[1], Hamed Saffari[2*], and Mohammad Javad Zahedi[3]

1. M.Sc. Student, Graduate University of Advanced Technology, Kerman, Iran
2. Professor, Shahid Bahonar University of Kerman, Iran,
* Corresponding Author; email: hsaffari@mail.uk.ac.ir
3. Ph.D. Student, Shahid Bahonar University of Kerman, Iran

Received: 20/07/2017
Accepted: 07/01/2018

ABSTRACT

The prediction of the seismic behavior of structures during earthquake has always been an important concern for earthquake and structural engineers. In addition to earthquakes, the behavior of soil and its effects on seismic responses of structure, also known as Soil-Structure Interaction (SSI), make this problem more complicated. For this purpose, today, many investigations are focusing on soil role in seismic behavior of structures. In this study, the seismic behavior of steel structures with various heights under the SSI effect have been studied. For this purpose, three steel structures including 9, 15 and 20 story frames were modeled using Opensees. Besides, their seismic behaviors under different base conditions including fixed base and on three different types of soil (B, C and D) under 11 bedrock earthquakes were also investigated using the direct method. The responses in two terms including story shear and story drift were also investigated.

Keywords:
Soil-Structure Interaction; Direct method; Moment resisting frame; Finite element; Opensees

1. Introduction

The prediction of seismic behavior of structures during earthquakes can significantly reduce fatalities and financial damages. Many efforts have been conducted by structural and earthquake engineers in order to find appropriate ways to enhance this knowledge. However, it is difficult to predict these behaviors due to the complexities of the nature of earthquakes. Aside from earthquakes, one of the most important parameters that should be considered is soil. Investigations show that the fixed base structure hypothesis, that is prevalent in calculating seismic responses of structures, is not reasonable when the soil under the structure is soft and flexible. It happens due to the inability of the foundation to conform to the free-field motion and the effect of structure on soil during ground motions [1].

The soil may significantly change final responses because it can increase damping and elongate the period of the considered system. The intensity of the soil-structure interaction effect on structural responses hinges on many parameters such as soil and structure relative stiffness and the slender ratio of structure. However, studies have been shown that structures with fundamental periods between 0.3 and 1 seconds are more sensitive in comparison with other structures [2]. Although, for those groups of structures that have been found on soil with shear wave velocity lower than 600 m/s, interaction between soil and structure may modify seismic responses more than other cases especially for moment resisting frames [3-4].

There are two conventional methods to solve

SSI problems [5]. The first approach is the direct method wherein the soil and structure elements are modeled as a unified system. The direct method is suitable in analyzing nonlinear and complex problems, but it is time-consuming and needs powerful processors for solving procedures. By use of this method, Karapetrou et al. [6] displayed the effects of soil depth and stratigraphy on the seismic response of concrete moment resisting structures. Krishnamoorthy and Anita [7] also studied the seismic responses of an isolated structure with linear elastic behavior considering soil-structure interaction using the direct method. In another study, Tabatabaiefar et al. [8] investigated the effect of soil-structure interaction on seismic behavior of mid-rise reinforced concrete moment resisting frames by using the FLAC2D programs. Matinmanesh and Saleh Asheghabadi [9] studied the effects of soil type, the frequency content of earthquake and the height of the structure on seismic responses of concrete frames. In another research, Tabatabaiefar and Massumi [10] analyzed the seismic behavior of reinforced concrete frames during four earthquakes considering soil-structure interaction using the direct method.

The second approach, named substructure method, calculates soil and structure responses separately and prepares the final results using the superposition principle. This method is faster than the direct method, but does not show good performance in nonlinear problems due to the nature of the superposition principle. To eliminate this limitation for shallow foundations, the beam on nonlinear Winkler foundation was introduced [11-13], which has shown acceptable performance in nonlinear problems. Rajeev and Tesfamariam [14], by the help of the substructure method, investigated the fragility curves of non-ductile reinforced concrete frames using the Opensee software and showed the effect of soil and foundation parameters on final responses of soil-structure system during different ground motions. In another study, Behnamfar and Banizade [15] analyzed the behavior of concrete structures with two different lateral load bearing systems (moment frame and shear wall systems) considering soil-structure interaction. Raychowdhury [16] used the substructure method to display the effects of soil parameters including cohesion, friction angle, shear modulus, Poisson's ratio, and unit weight on seismic responses of low rise steel frames. The substructure method was also used by Minasidis et al. [17] in order to determine fault mechanisms and SSI roles in seismic demands of steel moment resisting frames.

Recently, a new method named the macro element method was introduced to simulate soil-structure interaction problems. This approach was introduced by Nova and Montrasio [18] and used by Paolucci [19] for geotechnical problems for the first time. This method considers soil medium as divided by near and far-field. In this way, Grange et al. [20] introduced a macro element for shallow foundations, which could calculate the non-linear behavior of soil and the foundation uplift, to simulate the seismic behavior of soil-structure interaction models. The proposed macro element, after validation with parametric and experimental studies, showed suitable performance to model SSI problems. In another study, Grange et al. [21] used a macro element to obtain the seismic response of concrete viaducts under various soil conditions and showed the ability of the macro element method to solve these types of problems.

Aside from the mentioned approaches, data based methods were recently used by researchers as well. Farfani et al. [22] used Artificial Neural Networks and Support Vector Machines methods in order to model SSI and compared the obtained results with the outputs of Finite Element models. Pala et al. [23] studied the ability of Artificial Neural Networks to simulate soil-structure interaction problems too. They used outputs of the SAP2000 program to train, test and validate the mentioned networks. They showed that the data based method can also be useful in SSI problems.

There are also many experimental studies about SSI effects. Xiong et al. [24] investigated about the effects of structure to soil relative stiffness and mass ratio on structural responses using 1/4-scale steel frames. For this purpose, they studied the behavior of 34 frames (17 frames in two direction) with different values of mass and stiffness and measured the fundamental periods of structures. In another study, Hokmabadi et al. [25] studied the behavior of structures during three different base conditions (fixed base, shallow foundation and pile

foundation on soft soil) using laminar soil container and compared the results with numerical models.

In this study, the direct method was used to solve a soil-structure interaction problem. In this method, soils and structures are modeled as a unified system and analyzed simultaneously. Opensees [26], as a finite element software, was used to simulate a soil-structure problem. Three 2D steel moment resisting frames including 9, 15 and 20 story buildings have been modeled. Panel zones were modeled in the connection area between columns and beams and the nonlinearity of structure during earthquake was considered too. The soils were modeled as elastoplastic materials and appropriate boundary conditions were used to simulate the soil media. Finally, the seismic behavior of structures under 11 earthquakes and different base conditions was investigated through dynamic time history analyses. The results have been shown in two terms including story shear and story drift for all structures.

2. Numerical Modeling

2.1. Structures

Three steel moment resisting frames that have been designed by Karavasilis et al. [27] were used in this study. These structures include 9, 15 and 20 story two-dimensional frames with various section sizes. EC3 [28] and EC8 [29] were used to design these frames and gravity loads and yield stress of material were considered equal to 27.5 kN/m and 235 MPa, respectively. In addition, soil class B according to EC8 [29] and peak ground acceleration equal to 0.35 g were other assumptions in the design procedure. As a result, HEB and IPE sections with various dimensions were chosen for columns and beams, respectively. The mentioned structures have been modeled in three bay frames when the width of each bay is equal to 5 meters and typical height of stories has been assumed at 3 meters. Table (1) shows the characteristics of the structures:

For example, the meaning of 340-360 (1) is the columns of first story are HEB340 and the beams are IPE360.

Besides, Figure (1) shows the 9-story structure schematically.

In order to show the nonlinear behavior of structures, plastic hinges were considered. For this purpose, instead of original prismatic beam that has six degrees of freedom, a modified prismatic beam with eight degrees of freedom by help of two semi rigid rotational springs were used where the springs were modeled by Bilin material [30]. Figures (2) and (3) show the modified beam and the moment-rotation behavior of the Bilin material, respectively.

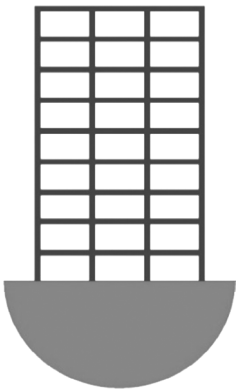

Figure 1. 9-story structure.

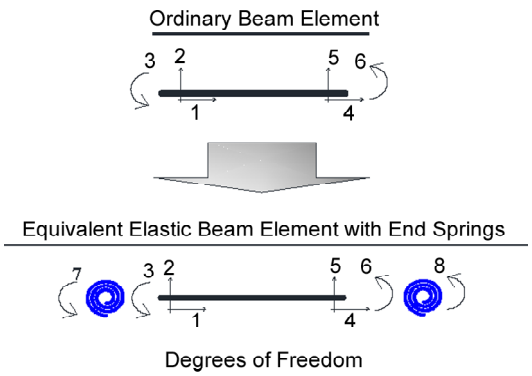

Figure 2. Modified prismatic beam with eight degree of freedoms.

Table 1. Characteristics of structures.

Frame	Story	Sections (Columns HEB – Beams IPE)
1	9	340–360(1)+340–400(2–5)+320–360(6–7)+300–330(8–9)
2	15	500–300(1) ⁞ 500–400(2–3) ⁞ 500–450(4–5) ⁞ 450–400(6–7) ⁞ 400–400(8–12) ⁞ 400–360–(13–14) ⁞ 400–330(15)
3	20	700–300(1)+700–360(2)+700–400(3)+700–450(4–5)+650–450(6–10)+600–450(11–13)+600–400(14–16)+ 550–400(17)+550–360(18–19)+550–330(20)

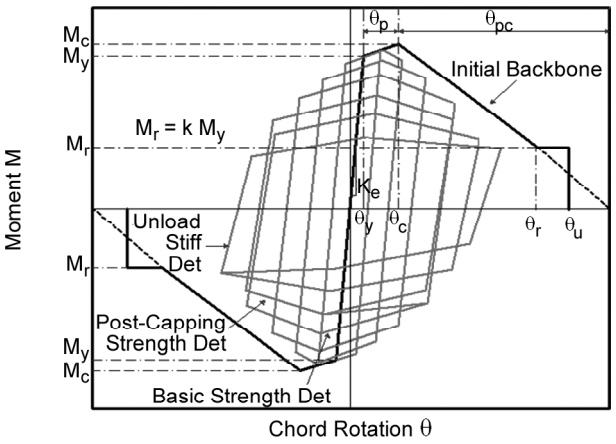

Figure 3. Moment-rotation behavior of Bilin material.

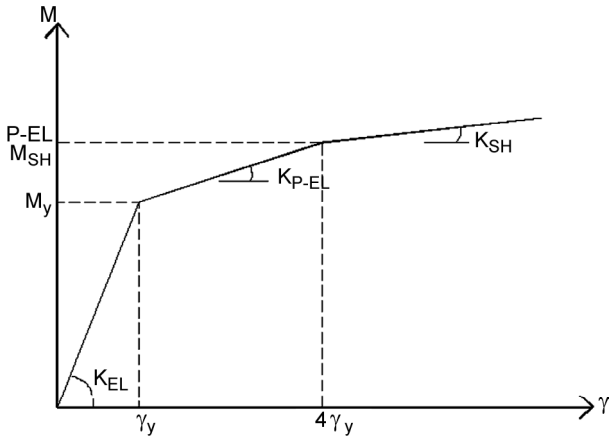

Figure 4. tri-linear behavior of panel zone.

The M_y, M_c and M_r parameters in Figure (3) indicate the effective yield strength moment, capping strength moment for monotonic loading and residual strength moment, respectively, when K_e is effective stiffness. In addition, effective yield rotation, capping rotation for monotonic loading, post capping rotation capacity, and ultimate rotation capacity have been shown with $\theta_y, \theta_y, \theta_{pc}$, and θ_u, respectively.

For making more realistic models, panel zones were modeled too. A panel zone is a quadrilateral area that is encompassed between the column web and the extension of beam flange line in connection point. Panel zone should transfer the moments between beams and columns and its role is more important when lateral loads are applied to structure. Mathematical relations to determine ultimate shear capacity and yield shear strength of panel zones were suggested in previous studies separately [31-34]. There are three prevalent models to simulate the behavior of panel zones. These models that show good conformability in elastic regions named bi-linear, tri-linear and quadric-linear models. The main difference between these models relates to the inelastic parts of them. In this study, tri-linear model has been used. Figure (4) shows the behavior of considered panel zone, where M_y and $M_{y,P-EL}$ are elastic and post-elastic yield moments of panel zone which are calculated by the following equations:

$$M_y = K_{EL}.\gamma \tag{1}$$

$$M_{y,P-EL} = A_v.d_b.\tau_y\left(1+\frac{3.12b_{fc}t_{fc}^{\ 2}}{A_v d_b}\right) \tag{2}$$

where A_v is shear area, τ_y is yield shear stress, d_b is the height of beam, and b_{fc} and t_{fc} are the width and thickness of column flange. K_{EL}, K_{P-EL} and K_{SH} are elastic, post-elastic and strain hardening stiffness, respectively.

The structure of panel zones was modeled using eight rigid elements with pinned connections and one rotational spring. Figure (5) shows considered panel zone schematically:

The foundation was not designed, and a beam with high rigidity was used to connect the structure to the soil. Between the mentioned beam and soil no interface element was used, and they were connected together by typical nodal connections based on previous researches [6, 35-36].

2.2. Soil Model

Soil is a semi-infinite half space that makes modeling it harder than other parts due to its special nature. The soil medium should prevent reflecting output waves towards the computing environment. Hence, boundary conditions play a crucial role in

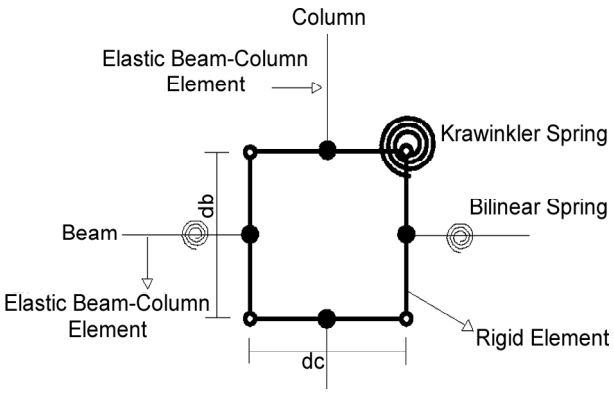

Figure 5. The modeled panel zone.

soil modeling. Various conditions were presented by different researchers in order to introduce a suitable boundary. For this purpose, Gutierrez and Chopra [37] used preliminary boundaries as lateral conditions. The main problem of these boundaries, which is obvious in dynamic analysis, is their disability to absorb output waves and depreciate them. Therefore, when using this boundary condition, in order to increase the accuracy, the dimensions of modeled soil should be increased, and it can significantly increase the volume of calculations. One of the more practical boundary conditions for lateral boundaries have been presented by Lysmer and Kuhlemeyer [38]. In this method, dashpots with a specified coefficient are used in order to reduce the volume of output wave reflection through dissipating them. White et al. [39] applied some changes in the Lysmer boundary coefficient and increased the ability of this type of boundary to absorb output waves. Besides, Zienkiewicz et al. [40] introduced a type of boundary wherein free-field columns were used. In addition, other boundary conditions like the infinite element and the kelvin element have been used as lateral boundaries [41-43]. According to previous studies, the rigid condition has been recognized as an appropriate assumption for the bottom boundary and many researchers used that for soil models [44-47]. In the soil modeling procedure, the dimensions of the soil medium is important, which also shares a direct relationship with boundary conditions. Ghosh and Wilson [48] in their studies, suggested a length and a depth for soil medium which were 3 to 4 times and 2 to 3 times of the foundation radius, respectively. In other investigations, Reyhani and El Naggar [49] concluded that using a distance which is at least equal to five times of the structure width can be appropriate. They also recommended a 30-meter depth for soil medium.

In this study, the depth of the basic soil model has been assumed as 30 meters and the distance of the lateral boundaries from each other are considered 10 times that of structure width. The thickness of soil model based on previous studies [50-51], was considered 5 meters. In this model, two free-field columns that are much thicker than soil medium were used as two lateral boundaries. Aside from that, the width of each column element is considered 5 times that of adjacent elements. The reason for the changes in the surrounding columns is to simulate the free-field behavior. Additionally, a Lysmer dashpot, in horizontal direction, was used in the bottom corner of soil model at the left side in order to account for the finite rigidity of the underlying half-space. The governing equations of this type of dashpots are:

$$\sigma = a\rho v_p \dot{w} \tag{3}$$

$$\tau = b\rho v_s \dot{u} \tag{4}$$

where σ, τ, v_p and v_s are normal stress, shear stress, velocity of P and S waves, respectively. $\dot{w}$ and $\dot{u}$ indicate normal and shear component of velocity at boundary and ρ is mass density of the material. a and b are two parameters whose duty is reducing reflected waves as much as possible and whose values depend on incident wave angles. Lysmer and Kuhlemeyer proposed 1 as the values of these parameters while the angles of incident waves are greater than 30 degrees.

The dimensions of soil model meshes, in order to increase the accuracy of calculations, were chosen so that the distance of any two nodes is not more than the obtained value out of the following equation [52]:

$$h \le \frac{v}{10 f_{\max}} \tag{5}$$

where h is the distance between two adjacent nodes, v is the lowest shear wave velocity and $f_{\max}$ is the highest relevant frequency of model. The value of $f_{\max}$ for this study has been considered equal to 10 based on previous study [52]. Besides, in order to increase the accuracy of the model, distances between the nodes became smaller, in both horizontal and vertical direction, when they approach to structure. Four-node elements, which have two degrees of freedom for each node, were used and the plain strain condition was considered.

In this study, three different types of soil (B, C and D based on Euro code) were used. Their properties have been shown in Table (2).

From Table (2), the values of the shear and bulk moduli were calculated based on the following equations:

$$G = \rho V^2 \tag{6}$$

$$B = \frac{(2G(1+\mu))}{3(1-2\mu)} \tag{7}$$

Table 2. Properties of soils.

Soil Type	Poisson Ratio (-)	Mass Density (Mg/m^3)	Shear Modulus (kN/m^2)	Bulk Modulus (kN/m^2)	Friction Angle (Degree)	Void Ratio (-)
B	0.28	2.1	525000.0	1018181.82	40	0.45
C	0.30	1.9	194560.0	421546.67	33	0.7
D	0.32	1.7	38250.0	93500.0	29	0.85

Table 3. Input motions.

Ground Motion Name	Station Name	Date	Radius (km)	Magnitude	Used Direction
Valneria	Cascia	19/09/1979	5	5.8	X
Lazio Abruzzo	Atina	07/05/1984	5	5.9	X
Izmit (After Shock)	Izmit-Meteoroloji Istasyonu	13/09/1999	15	5.8	X
Kozani	Kozani-Prefecture	13/05/1995	17	6.5	Y
Montenegro	Ulcinj-Hotel Albatros	15/04/1979	21	6.9	X
Valneria	Arquata del Tronto	19/09/1979	22	5.8	X
Lazio Abruzzo	Ponte Corvo	07/05/1984	22	5.9	X
Friuli	Tolmezzo-Diga Ambiesta	06/05/1976	23	6.5	X
Compano Lucano	Bagnoli-Irpino	23/11/1980	23	6.9	X
Golbasi	Golbasi-Devlet Hastanesi	05/05/1986	29	6	Y
Montenegro (After Shock)	Hercegnovi Novi-O.S.D. Pavicic School	24/05/1979	30	6.2	X

where G and B are shear and bulk moduli and τ, V and μ indicate mass density, shear wave velocity and Poisson's ratio, respectively.

3. Input Motions

For this study, 11 different ground motions were used as input motions. These ground motions were selected from a previous work [53] and downloaded on the European Strong-Motion Database (http://www.isesd.hi.is). Table (3) shows the properties of ground motions.

Table (3) shows that the selected ground motions have a magnitude range between 5.8 and 6.9 and ranging radiuses from 5 to 30 km. For seismic analysis, the Peak Ground Accelerations (PGAs) of all these motions were scaled to 0.3 g. After that, ground motions were applied to models in three different conditions:

1. For the first condition, all scaled motions were applied to the base of the fixed base structures directly. This means that there is no soil model and structures have been found on hard rock (fix).
2. In the second condition, all of the scaled ground motions were filtered by modeled soil media. Afterwards, obtained acceleration time histories at the top of the soils were used as input motions for the fixed base structures. This procedure reveals the site effects on the structural responses (soil type - fix).
3. In the third and final condition, structures and soils were modeled, and scaled ground motions were applied at the bottom of soil media. In this condition, the complete SSI effect can be studied (soil type-SSI).

Figure (6) shows different conditions for applying input motions to structures.

The dynamic analyses of SSI models, under mentioned conditions, were conducted and results have been reported in the following sections.

4. Model Validation

The response of the soil model was compared with the obtained result out of a centrifuge test which was conducted by Hashash et al. [54]. For this purpose, the condition of a certain soil under the Loma Prieta earthquake was simulated by Hashash et al. [54] and the surface Pesudo Spectral Acceleration (PSA) of that has been compared with the corresponding value of the numerical model, which was used in this study. The soil parameters of the Opensees model have been shown in Table (4).

Figure (7) shows the comparison between the obtained PSA out of the centrifuge test and Opensees model. As it is obvious, the output of numerical model displayed good accordance with the result of experimental test.

In other case, a real event was investigated and

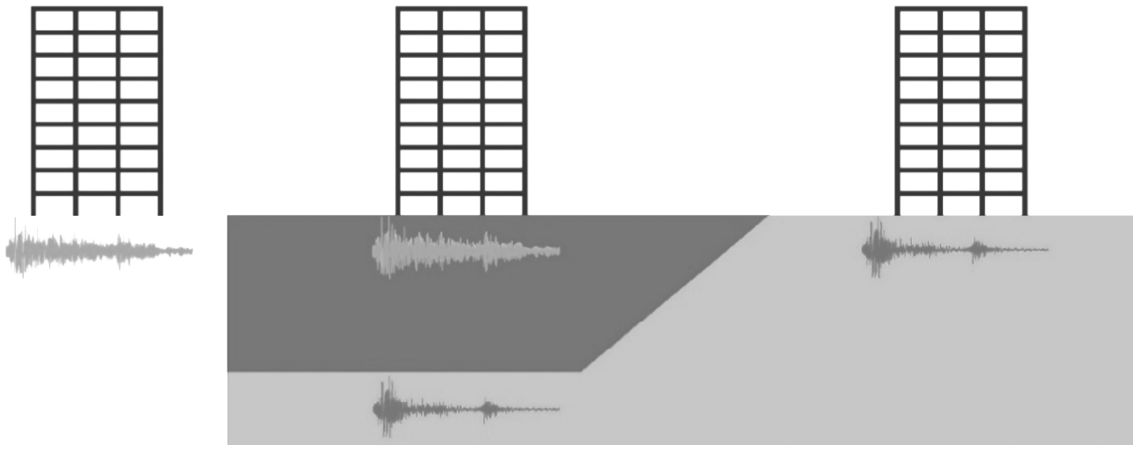

Figure 6. Different conditions of the analysis.

Table 4. The modeled soil used by Hashash et al [54].

Variable (Unit)	Value
Poisson's Ratio (-)	0.31
Mass Density (Mg/m^3)	1.56
Shear Modulus (KN/m^2)	82900
Bulk Modulus (KN/m^2)	191000
Friction Angle (degree)	33
Void Ratio (-)	0.692
Soil Depth (m)	26

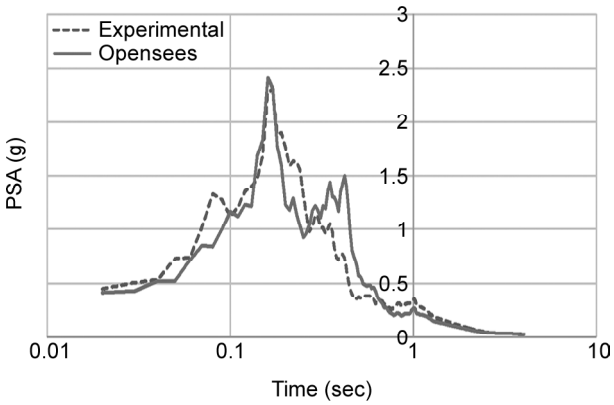

Figure 7. Comparison between experimental and Opensees outputs.

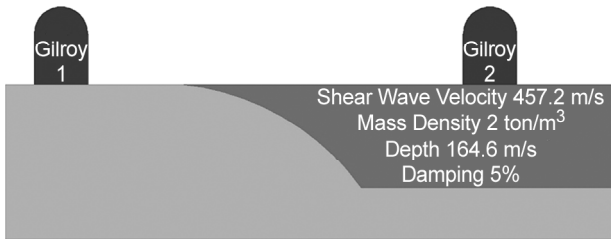

Figure 8. Base conditions in Gilroy 1 and Gilroy 2 stations.

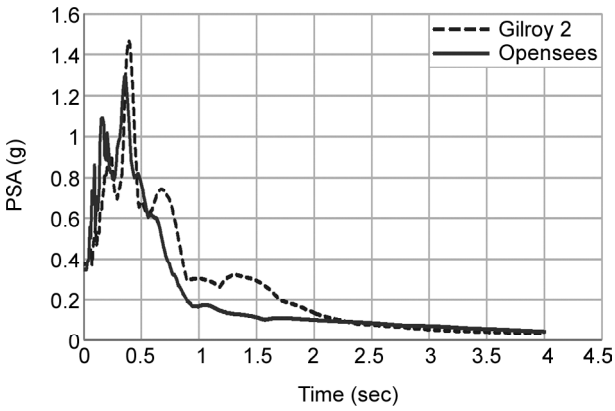

Figure 9. Comparison between real event and Opensees outputs.

the results of that were compared with the simulated output of soil model. For this purpose, the information of Gilroy 1 and Gilroy 2 stations were used. The Gilroy 1 station has recorded the Loma Prieta earthquake data from the bedrock while Gilroy 2 station did that on the soil layers. For modeling, the equivalent soil layer data was obtained from the previous study [1]. Situations of the stations have been shown in Figure (8) schematically. The soil surface PSAs of the Opensees model and Gilroy 2 station have been shown in Figure (9).

The results show good behavior for simulated soil media and displays suitable accuracy.

5. Results and Discussion

5.1. Site Effect on Input Motion

At first, a comparison was conducted to show the effect of different soil media on the input motions. For this purpose, 0.3 g scaled motions were applied to the bottom of different soil media and the PSAs on the surface of each medium were recorded. Finally, the average value of the surface

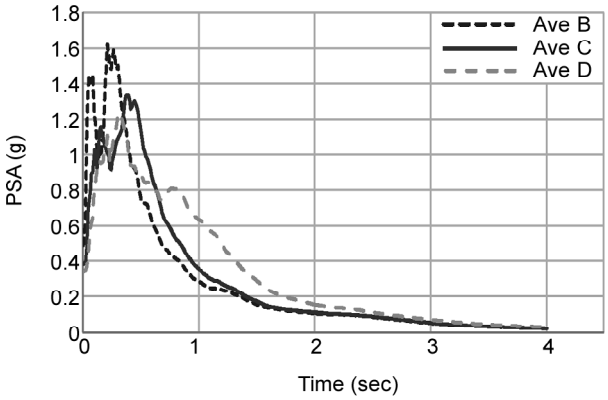

Figure 10. Average of pseudo spectral accelerations on the surface of each soil.

PSAs for each soil were calculated. Figure (10) shows the average of pseudo spectral accelerations on the surface of each soil.

Figure (10) shows that the maximum value of PSA happened in harder soil (soil B) and the minimum value occurred at soft soil (soil D). It is also obvious that when the soil became softer, the larger value could be observed for higher periods. Table (5) shows the maximum of pseudo spectral accelerations and peak ground accelerations for different conditions.

Table (5) shows that the values of PGA and maximum PSA have decreased by soil softening. This phenomenon can be justified by the concept of soil damping and stiffness. Softer soil has lower stiffness and consequently shows higher damping ability and because of that, it can dissipate the energy of input motions more than harder soil. Results obviously show that how the softer soil increase the effective period domain of PSA.

5.2. Structural Story Shear

One of the most important parameters in structural design is the story shears of the structure. For this reason, the values of story shears for different structures under the mentioned conditions for input motions were calculated. Finally, the average of story shear values for each one of conditions were reported through Figures (11) to (13).

Figures (11) to (13) show that when the scaled input motion without site and SSI effects are used (first case), the obtained story shears were lower than that for other conditions. Additionally, when the second (site effect) and third (SSI effect) cases were compared, the results showed that the values of story shears decreases when the SSI is completely calculated in comparison with the corresponding values when only the site effect is considered. Table (6) shows the reduction factors of base shears for different soils and structures.

Table 5. Maximum of PSA and PGA values of different soil condition.

Motion Type	Maximum PSA	Maximum PSA Period	PGA
B surface	1.62	0.21	0.49
C surface	1.33	0.39	0.38
D surface	1.23	0.31	0.33

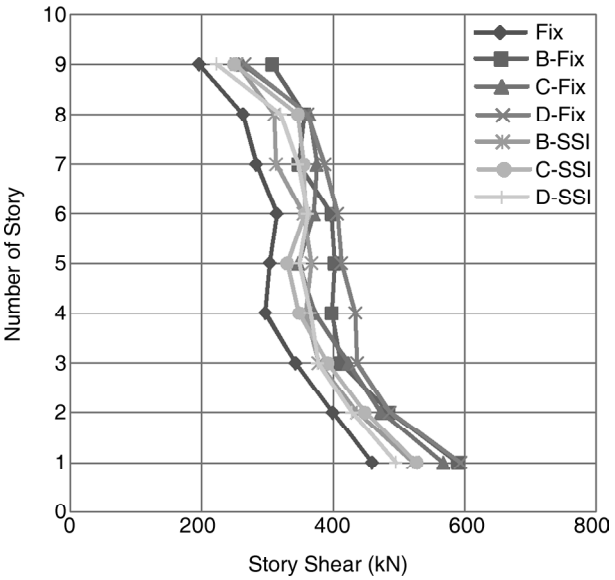

Figure 11. Story shear values for 9-story structure in different conditions.

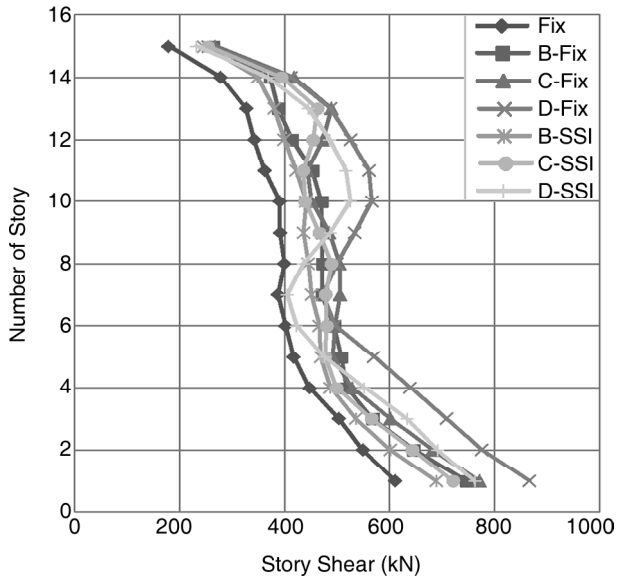

Figure 12. Story shear values for 15-story structure in different conditions.

Table 6. Reduction factors of base shears.

Structure	Soil B	Soil C	Soil D
9 story	0.88	0.92	0.83
15 story	0.92	0.93	0.87
20 story	0.91	0.88	0.84

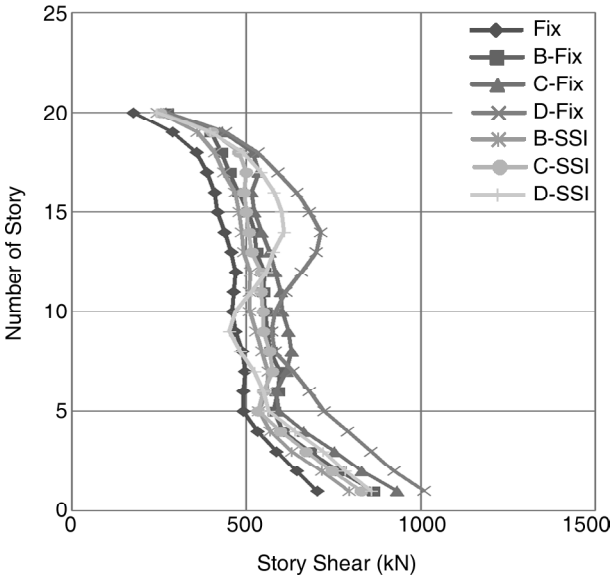

Figure 13. Story shear values for 20-story structure in different conditions.

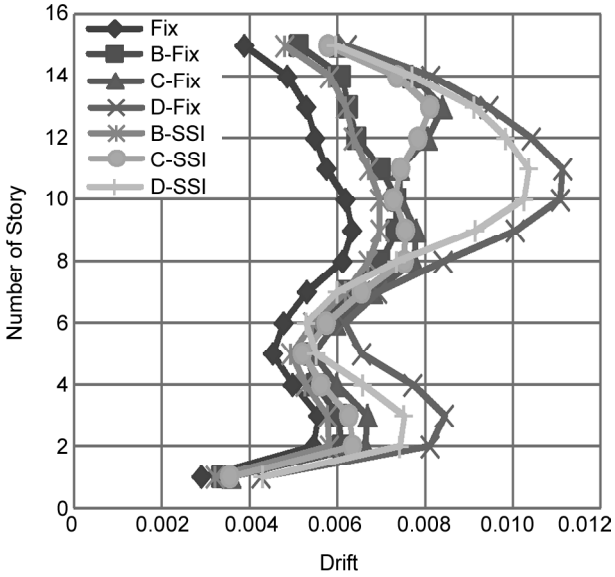

Figure 15. Drift values for 15-story structure in different conditions.

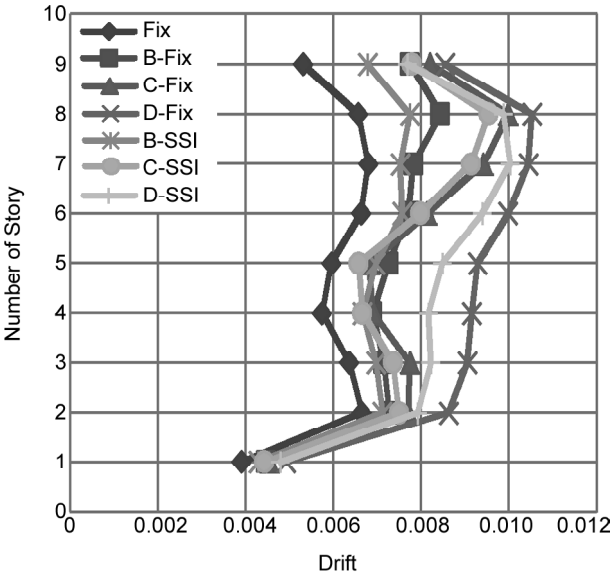

Figure 14. Drift values for 9-story structure in different conditions.

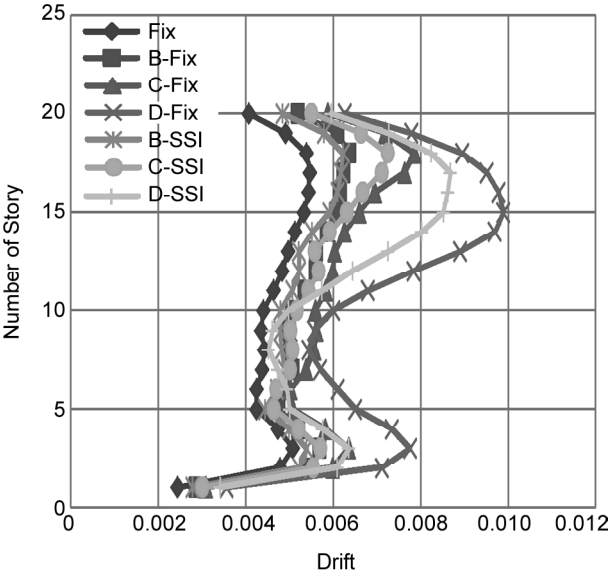

Figure 16. Drift values for 20-story structure in different conditions.

5.2. Story Drift

Another important parameter for designers is drift. Drift is the relevant angle between adjacent floors. Drift values in this study have been calculated based on the following equation:

$$drift = \frac{\Delta_{i+1} - \Delta_i}{h} \quad (8)$$

where Δ_{i+1} and Δ_i are the displacement of upper and lower floors, respectively, and h is the height of story. It should be noted that the effects of rocking were not removed and the mentioned values for drifts include it. Figures (14) to (16) show obtained drifts out of different conditions:

Results show that the drift values in the first case

are minimum. This was predictable, as shown in Figure (10), that soil can intensify the bedrock motion significantly. After the comparison between the second and third cases, it was determined that the drift values out of the site effect case are mostly higher than the corresponding values for SSI cases. The drift ratio depends on the combination of base shear and rocking effects. In the presence of soil, base shear mostly decreases while rocking increases. In these models, it seems that the effect of base shear reduction was more than rocking and because of that the SSI models have been shown lower drifts. It is also obvious that the maximum drifts have increased when the soil became softer. This shows that the consideration of SSI is more important for softer soils.

6. Conclusion

In this study, three steel structures with different heights were analyzed during eleven ground motions and their seismic behaviors in two different terms including structural drift and story shear have been reported. Panel zones were modeled to increase the model accuracy and different conditions have been considered for the base of structures. The following results have been concluded in this study:

- When the soil became softer, the corresponding PGA have decreased. It could happen due to the reduction of stiffness that usually leads to more damping. Besides, it was obvious that softer soil increase the effective period domain of PSA.
- In all cases, it was obvious that the drifts have increased when the soil became softer. As shown in the graphs, soil D shows the greatest values of drifts for all structures and after that soil C and soil B were located, respectively. It may justify by increasing the base shear and rocking when the soil become softer. All studied structures had fundamental period in the area that softer soils show greater PSAs, and it is expected that softer soil makes greater base shears.
- Changing the soil type can also modify the drift pattern and it is more obvious for taller structures. Soil D made greater range of drift values for different floors of a certain structure and it was more obvious for taller structures.
- During the study about different base conditions, all demands show a reduction during SSI conditions in comparison with the corresponding fixed base models, but minimum values belonged to the fixed base model with bedrock motion. This shows that in the same condition, using the bedrock motion is not suitable for a structure when it has been found on soft soil.
- This study showed that considering soil-structure interaction can be beneficial in some cases and could reduce seismic demands and subsequently lead to more affordable designs.

References

1. Kramer, S.L. (1996) *Geotechnical Earthquake Engineering*. Prentice Hall Civil Engineering and Engineering Mechanics Series.
2. Dutta, S.C., Bhattacharya, K. and Roy, R. (2004) Response of low-rise buildings under seismic ground excitation incorporating soil-structure interaction. *Soil Dynamics and Earthquake Engineering*, **24**, 893-914.
3. Veletsos A.S. and Meek J.W. (1974) Dynamic behaviour of building-foundation systems. *Earthquake Engineering & Structural Dynamics*, **3**, 121-138.
4. Galal, K. and Naimi, M. (2008) Effect of soil conditions on the response of reinforced concrete tall structures to near-fault earthquakes. *The Structural Design of Tall and Special Buildings*, **17**, 541-562.
5. Wolf, J.P. (1985) *Dynamic Soil Structure Interaction*. NewJersey, Prentice Hall.
6. Karapetrou, S., Fotopoulou, S., and Pitilakis, K. (2015) Seismic vulnerability assessment of high-rise non-ductile RC buildings considering soil-structure interaction effects. *Soil Dynamics and Earthquake Engineering*, **73**, 42-57.
7. Krishnamoorthy, A. and Anita, S. (2016) Soil-structure interaction analysis of a FPS-isolated structure using finite element model. *Structures*, **5**, 44-57.
8. Tabatabaiefar, H.R., Fatahi, B., and Samali, B. (2013) Lateral seismic response of building frames considering dynamic soil-structure interaction effects. *Structural Engineering and*

Mechanics, **45**, 311-321.

9. Matinmanesh, H. and Asheghabadi, M.S. (2011) Seismic analysis on soil-structure interaction of buildings over sandy soil. *Procedia Engineering*, **14**, 1737-1743.

10. Tabatabaiefar, H.R. and Massumi, A. (2010) A simplified method to determine seismic responses of reinforced concrete moment resisting building frames under influence of soil-structure interaction. *Soil Dynamics and Earthquake Engineering*, **30**, 1259-1267.

11. Harden, C.W., Hutchinson, T., Martin, G.R., and Kutter, B.L. (2005) *Numerical Modeling of the Nonlinear Cyclic Response of Shallow Foundations*. Pacific Earthquake Engineering Research Center, PEER.

12. Raychowdhury, P. (2008) *Nonlinear Winkler-based Shallow Foundation Model for Performance Assessment of Seismically Loaded Structures*. University of California, San Diego.

13. Raychowdhury, P. and Hutchinson, T.C. (2009) Performance evaluation of a nonlinear Winkler-based shallow foundation model using centrifuge test results. *Earthquake Engineering and Structural Dynamics*, **38**, 679-698.

14. Rajeev, P. and Tesfamariam, S. (2012) Seismic fragilities of non-ductile reinforced concrete frames with consideration of soil structure interaction. *Soil Dynamics and Earthquake Engineering*, **40**, 78-86.

15. Behnamfar, F. and Banizadeh, M. (2016) Effects of soil-structure interaction on distribution of seismic vulnerability in RC structures. *Soil Dynamics and Earthquake Engineering*, **80**, 73-86.

16. Raychowdhury, P. (2009) Effect of soil parameter uncertainty on seismic demand of low-rise steel buildings on dense silty sand. *Soil Dynamics and Earthquake Engineering*, **29**(10), 1367-1378.

17. Minasidis, G., Hatzigeorgiou, G., and Beskos, D. (2014) SSI in steel frames subjected to near-fault earthquakes. *Soil Dynamics and Earthquake Engineering*, **66**, 56-68.

18. Nova, R. and Montrasio, L. (1991) Settlements of shallow foundations on sand. *Géotechnique*, **41**, 243-256.

19. Paolucci, R. (1997) Simplified evaluation of earthquake-induced permanent displacements of shallow foundations. *Journal of Earthquake Engineering*, **1**(03), 563-579.

20. Grange, S., Kotronis, P., and Mazars, J. (2009) A macro-element to simulate dynamic soil-structure interaction. *Engineering Structures*, **31**, 3034-3046.

21. Grange, S., Botrugno, L., Kotronis, P., and Tamagnini, C. (2011) The effects of soil-structure interaction on a reinforced concrete viaduct. *Earthquake Engineering & Structural Dynamics*, **40**, 93-105.

22. Farfani, H.A., Behnamfar, F., and Fathollahi, A. (2015) Dynamic analysis of soil-structure interaction using the neural networks and the support vector machines. *Expert Systems with Applications*, **42**, 8971-8981.

23. Pala, M., Caglar, N., Elmas, M., Cevik, A., and Saribiyik, M. (2008) Dynamic soil-structure interaction analysis of buildings by neural networks. *Construction and Building Materials*, **22**(3), 330-342.

24. Xiong, W., Jiang, L.Z., and Li, Y.Z. (2016) Influence of soil-structure interaction (structure-to-soil relative stiffness and mass ratio) on the fundamental period of buildings: experimental observation and analytical verification. *Bulletin of Earthquake Engineering*, **14**, 139-160.

25. Hokmabadi, A.S., Fatahi, B., and Samali, B. (2014) Seismic response of mid-rise buildings on shallow and end-bearing pile foundations in soft soil. *Soils and Foundations*, **54**, 345-363.

26. OpenSees (2013) Open system for earthquake engineering simulation. PEER, http://opensees.berkeley.edu, Richmond, CA, USA.

27. Karavasilis T.L., Bazeos, N., and Beskos, D.E. (2007) Behavior factor for performance-based seismic design of plane steel moment resisting frames. *Journal of Earthquake Engineering*,

11, 531-559.

28. EC3 - EN 1993-1-1. Eurocode 3 (1993) Design of Steel Structures. *Part 1-1: General Rules and Rules for Buildings*. European committee for standardization (CEN), Brussels.

29. EC8 - EN 1998-1. Eurocode 8 (2005) Design of Structures for Earthquake Resistance; *Part 1: General Rules*. Seismic Actions and Rules for Buildings. European Committee for Standardization, Brussels.

30. Lignos, D., Krawinkler, H., and Whittaker, A. (2011) Prediction and validation of sidesway collapse of two scale models of a 4-story steel moment frame. *Earthquake Engineering & Structural Dynamics*, **40**, 807-825.

31. Krawinkler, H. (1971) *Inelastic Behavior of Steel Beam-to-Column Subassemblages*. Vol. 71. University of California, Berkeley.

32. Krawinkler, H. and Mohasseb, S. (1987) Effects of panel zone deformations on seismic response. *Journal of Constructional Steel Research*, **8**, 233-250.

33. Mansouri, I. and Saffari, H. (2014) A new steel panel zone model including axial force for thin to thick column flanges. *Steel and Composite Structures*, **16**, 417-436.

34. Saffari, H., Sarfarazi, S., and Fakhraddini, A. (2016) A mathematical steel panel zone model for flanged cruciform columns. *Steel and Composite Structures*, **20**, 851-867.

35. Karimi, Z. and Dashti, S. (2015) Numerical and centrifuge modeling of seismic soil-foundation-structure interaction on liquefiable ground. *Journal of Geotechnical and Geoenvironmental Engineering*, **142**, 04015061.

36. Karimi, Z. and Dashti, S. (2016) Seismic performance of shallow founded structures on liquefiable ground: validation of numerical simulations using centrifuge experiments. *Journal of Geotechnical and Geoenvironmental Engineering*, **142**, 04016011.

37. Gutierrez, J.A. and Chopra, A.K. (1978) A substructure method for earthquake analysis of structures including structure-soil interaction. *Earthquake Engineering and Structural Dynamics*, **6**, 51-69.

38. Lysmer, J. and Kuhlemeyer, R.L. (1969) Finite dynamic model for infinite media. *Journal of the Engineering Mechanics Division*, **95**, 859-878.

39. White, W., Lee, I.K., and Valliappan, S. (1977) Unified boundary for finite dynamic models. *Journal of the Engineering Mechanics Division*, **103**, 949-964.

40. Zienkiewicz, O., Bicanic, N., and Shen, F. (1989) *Earthquake Input Definition and the Transmitting Boundary Conditions*. Advances in Computational Nonlinear Mechanics, 109-138.

41. Bentley, K.J. and Naggar, M.H.E. (2000) Numerical analysis of kinematic response of single piles. *Canadian Geotechnical Journal*, **37**, 1368-1382.

42. Maheshwari, B.K., Truman, K.Z., El Naggar, M.H., and Gould, P.L. (2004) Three-dimensional finite element nonlinear dynamic analysis of pile groups for lateral transient and seismic excitations. *Canadian Geotechnical Journal*, **41**(1), 118-133.

43. Zhao, C. and Valliappan, S. (1993) A dynamic infinite element for three-dimensional infinite-domain wave problems. *International Journal for Numerical Methods in Engineering*, **36**, 2567-2580.

44. Dutta, S.C. and Roy, R. (2002) A critical review on idealization and modeling for interaction among soil-foundation-structure system. *Computers and Structures*, **80**, 1579-1594.

45. Kocak, S. and Mengi, Y. (2000) A simple soil-structure interaction model. *Applied Mathematical Modelling*, **24**, 607-635.

46. Spyrakos, C., Maniatakis, C.A., and Koutromanos, I. (2009) Soil-structure interaction effects on base-isolated buildings founded on soil stratum. *Engineering Structures*, **31**, 729-737.

47. Zheng, J. and Takeda, T. (1995) Effects of soil-structure interaction on seismic response of PC cable-stayed bridge. *Soil Dynamics and*

Earthquake Engineering, **14**, 427-437.

48. Ghosh, S. and Wilson, E. (1969) *Dynamic Stress Analysis of Axisymmetric Structures under Arbitrary Loading*. University of California, Berkeley.

49. Rayhani, M. and El Naggar, M.H. (2008) Numerical modeling of seismic response of rigid foundation on soft soil. *International Journal of Geomechanics*, **8**, 336-346.

50. Saez, E., Lopez-Caballero, F. and Modaressi-Farahmand-Razavi, A. (2011) Effect of the inelastic dynamic soil-structure interaction on the seismic vulnerability assessment. *Structural Safety*, **33**, 51-63.

51. Saez, E., Lopez-Caballero, F., and Modaressi-Farahmand-Razavi, A. (2013) Inelastic dynamic soil-structure interaction effects on moment-resisting frame buildings. *Engineering Structures*, **51**, 166-177.

52. Jeremic, B., Jie, G., Preisig, M., and Tafazzoli, N. (2009) Time domain simulation of soil-foundation-structure interaction in non-uniform soils. *Earthquake Engineering and Structural Dynamics*, **38**, 699.

53. Pitilakis, K., Karapetrou, S., and Fotopoulou, S. (2014) Consideration of aging and SSI effects on seismic vulnerability assessment of RC buildings. *Bulletin of Earthquake Engineering*, **12**, 1755-1776.

54. Hashash, Y.M., Dashti, S., Romero, M.I., Ghayoomi, M., and Musgrove, M. (2015) Evaluation of 1-D seismic site response modeling of sand using centrifuge experiments. *Soil Dynamics and Earthquake Engineering*, **78**, 19-31.